⌘ *Author's Choice*

THE JOURNAL OF BIOLOGICAL CHEMISTRY VOL. 286, NO. 28, pp. 24987–24995, July 15, 2011

Characterization of G2L3 (GAS2-like 3), a New Microtubule- and Actin-binding Protein Related to Spectraplakins*[S]

Received for publication, March 23, 2011, and in revised form, May 5, 2011 Published, JBC Papers in Press, May 11, 2011, DOI 10.1074/jbc.M111.242263

Matthew J. Stroud, Richard A. Kammerer[1,2], and Christoph Ballestrem[1,3]

From the Wellcome Trust Centre for Cell-Matrix Research, Faculty of Life Sciences, University of Manchester, Manchester M13 9PT, United Kingdom

The microtubule (MT) and actin cytoskeletons are fundamental to cell integrity, because they control a host of cellular activities, including cell division, growth, polarization, and migration. Proteins involved in mediating the cross-talk between MT and actin cytoskeletons are key to many cellular processes and play important physiological roles. We identified a new member of the GAS2 family of MT-actin cross-linking proteins, named G2L3 (GAS2-like 3). We show that GAS2-like 3 is widely conserved throughout evolution and is ubiquitously expressed in human tissues. GAS2-like 3 interacts with filamentous actin and MTs via its single calponin homology type 3 domain and C terminus, respectively. Interestingly, the role of the putative MT-binding GAS2-related domain is to modulate the binding of GAS2-like 3 to both filamentous actin and MTs. This is in contrast to GAS2-related domains found in related proteins, where it functions as a MT-binding domain. Furthermore, we show that tubulin acetylation drives GAS2-like 3 localization to MTs and may provide functional insights into the role of GAS2-like 3.

The cytoskeleton is fundamental to cellular integrity, providing a molecular framework for both mechanical support and an intracellular transport infrastructure (1). Until recently, the microtubule (MT)[4] and actin cytoskeletons have been investigated as separate entities; however, it has become clear that they function in an interdependent way (2, 3). For example, MTs use filamentous actin (F-actin) to guide them from the cell interior to focal adhesions at the cell periphery (4). Understanding how the two components interact will therefore be key to our further understanding of fundamental cellular processes, such as cell division, growth, polarization, and migration.

The spectraplakins are a well characterized example of a protein family that can cross-link MT and actin cytoskeletons (5). There are two members expressed in mammals, microtubule-actin cross-linking factor 1 (MACF1 or ACF7), and bullous pemphigoid antigen 1, both of which are huge, multidomain-containing proteins (>500 kDa in mass) with binding sites for both F-actin via their calponin homology (CH) domains and MTs via their GAS2-related (GAR) domain and/or GSR repeats. Ablation of the ACF7 gene in mice results in embryonic lethality. However, $ACF7^{-/-}$ cells can be derived from the embryo and display defects in MT dynamics, guidance, cortical tethering, stability, and cellular polarization (3). Accordingly, various medical conditions and developmental defects arise as a result of mutations in genes encoding spectraplakins, including mental retardation, cancer, and chronic skin blistering (6), underlining the importance of proteins that link the actin and MT cytoskeletons.

Whereas the role of spectraplakins in cross-linking the MT and actin cytoskeletons is well established (3, 4, 7), the functions of the related GAS2 family remain to be determined. The GAS2 family can be thought of as mini-versions of spectraplakins, because they too contain a putative actin-binding CH domain and a putative MT-binding GAR domain. Interestingly, the expression of a mini-version of ACF7 consisting of the CH and GAR domains is sufficient to rescue these perturbations in function, implying that these are the key functional domains of spectraplakins (3). The first identified member of the GAS2 cross-linking family, termed GAS2, was originally identified in a screen looking for genes induced by growth arrest (8). GAS2 localizes along actin stress fibers, and GAS2 phosphorylation is coupled to rearrangements of actin in G_0 to G_1 transition (9, 10). There is some evidence to suggest that it may also be involved in apoptosis and tumor suppression (10–12). Two related family members were identified either in a search for putative tumor suppressors (hGAR22 (human Gas2-related gene on chromosome 22) or G2L1 (GAS2-like 1)) or by sequence similarity to hGAR22 (hGAR17 (human Gas2-related gene on chromosome 17) or G2L2 (GAS2-like 2)) (2, 13). Both transcripts encoding the respective proteins are subject to alternative splicing, which results in proteins with different localization and binding properties. The shorter isoforms, termed hG2L1α and hG2L2α, predominantly localize to the actin cytoskeleton and interact with F-actin *in vitro*. Conversely, both of the longer isoforms, termed hG2L1β and hG2L2β, localize and bind to both F-actin and MTs (2), suggesting that they may play a role in mediating cross-talk between the cytoskeletal systems.

* This work was supported by a Wellcome Trust Ph.D. studentship (to M. J. S.), a Wellcome Trust Senior Research Fellowship ((080878/Z/06/Z), to R. A. K.), and Biotechnology and Biological Sciences Research Council Grant BB/G004552/1 (to C. B.).

⌘ *Author's Choice*—Final version full access.

[S] The on-line version of this article (available at http://www.jbc.org) contains supplemental Table S1.

[1] Both authors contributed equally to this work.

[2] To whom correspondence may be addressed. Present address: Laboratory of Biomolecular Research, OFLC 106, Paul Scherrer Institut, CH-5232 Villingen PSI, Switzerland. E-mail: richard.kammerer@psi.ch.

[3] To whom correspondence may be addressed. E-mail: christoph.ballestrem@manchester.ac.uk.

[4] The abbreviations used are: MT, microtubule; F-actin, filamentous actin; CH, calponin homology; GAR, GAS2-related; MACF, microtubule-actin cross-linking factor; TSA, trichostatin A; FRAP, fluorescence recovery after photobleaching; AA, amino acid.

In the present study, we describe the characterization of a new family member, G2L3 (GAS2-like 3), which has the potential to communicate between MTs and actin. G2L3 is widely conserved through evolution, and it is abundant in most human tissues and the majority of cell lines that we tested. Full-length G2L3 interacts with both F-actin and MTs in cells and *in vitro* via its CH domain and C terminus, respectively. A third domain, termed the GAR domain, does not directly bind to F-actin or MTs; however, it is involved in modulating the binding strength of G2L3 to each cytoskeletal system. Interestingly, we found that acetylation of α-tubulin contributes to the recruitment of G2L3 to MTs.

EXPERIMENTAL PROCEDURES

Cell Culture and Transfections—All cells were grown in DMEM (Sigma-Aldrich) supplemented with 10% FBS and 1% glutamine in a 5% CO_2 in a humidified incubator and passaged in a 1:10 dilution every 3 days. For transfections, the cells were plated in six-well dishes a day before transfections. For transient transfections, 1–1.5 μg of DNA in total was transfected into cells using Lipofectamine Plus (Invitrogen) in accordance with the manufacturer's instructions. The cells were replated after 3 h in glass-bottomed dishes (MatTek Corporation, Ashland, MA) coated with 10 μg/ml bovine fibronectin (Sigma). For drug treatments, the cells were incubated for 30 min with either nocodazole (10 μM), cytochalasin D (2 μM), or trichostatin A (TSA) (5 μM) (all from Sigma).

Immunofluorescence Imaging—The cells were fixed and permeabilized with 3% paraformaldehyde (Sigma) containing 0.25% Triton X-100 (Sigma) and 0.05% glutaraldehyde (Sigma) for 15 min, before being washed in PBS (Lonza, Verviers, Belgium). Autofluorescence from reactive amine groups was quenched using 0.01% sodium tetrahydroborate (Sigma) in PBS for 15 min before being washed in PBS. Subsequently the cells were incubated for 45 min with anti-tubulin or anti-acetylated tubulin antibodies at 1:500 dilution (DM1A and 6-11B-1, respectively; Sigma), followed by three washes with PBS. Secondary antibodies conjugated to Cy2, Cy3, or Cy5 (Jackson ImmunoResearch Laboratories, Suffolk, UK) were then applied for 30 min. In the case of colabeling for actin, Texas Red or FITC-labeled phalloidin (Invitrogen) was added together with the secondary antibody). The cells were then washed three more times in PBS before being imaged using an oil-immersed 100× objective, with 1.35 numerical aperture on an inverted microscope (IX71; Olympus) controlled by a Deltavision system (Applied Precision, Issaquah, WA). Images were captured using a Coolsnap HQ CCD camera (Princeton Instruments, Lurgan, UK).

Fluorescence Recovery after Photobleaching (FRAP)—An inverted microscope (IX70) equipped with a 488-nm laser line (Olympus) under the control of software (DeltaVisionRT) were used for FRAP experiments. Cells plated on glass-bottomed dishes and expressing the indicated GFP-tagged constructs were imaged at 37 °C in Ham's F-12 medium (Sigma). 1.5-μm-diameter regions of interest were selected. Half-times of recovery were calculated using softWoRx FRAP analysis suite (see application notes at the Applied Precision website). Upon point bleaching, there is a natural occurrence of bleaching outside the region of interest. This is automatically adjusted for by the softWoRx suite (Applied Precision), which normalizes the fluorescence intensity readings to adjacent background levels and enables accurate readings to be measured. For image display, we have now adjusted the brightness of the individual time points accordingly. When performing FRAP on G2L3-expressing cells, we selected subcellular areas where G2L3 localized to either actin filaments (see Fig. 4*A*) or MTs (see Fig. 4*B*).

Image Processing—The images were processed using ImageJ version 1.43R. To quantify subcellular G2L3 localization, cells were selected at random, and G2L3 localization was scored as either diffuse, to actin alone, to MTs alone, or to both MTs and actin (see Fig. 5*B*). For colocalization studies and calculation of the ratio of GAS2-like 3/MTs for TSA analysis, images were background-subtracted using a two-dimensional bandpass filter, and overlay images were created. From these, a threshold was set to restrict analyses to MTs, and the outline of the cell was drawn followed by measuring the percentage area of positive pixels. This was repeated for GAS2-like 3 and divided by the value given for MTs to give a ratio theoretically between 0 and 1 (see Fig. 6*C*). Adobe Photoshop CS4 was used in the preparation of figures for this manuscript.

cDNA Panels—To identify human tissue expression, a "master mix" containing forward and reverse primers, dNTPs, reaction buffer, and *Taq* polymerase was made for cDNA panels (Clontech). cDNA libraries from various cell lines were made using the Absolutely RNA microprep kit followed by the Stratascript QPCR cDNA synthesis kit (Stratagene, Cheshire, UK) according to the manufacturer's recommendations. A master mix was also made to identify expression in the cell lines HeLa, human foreskin fibroblasts, HT1080, HEK293T, and murine NIH 3T3. The total reaction volume for each reaction was 25 μl; the reactions were incubated at 94 °C for 1 min, followed by 35 cycles of 30 s at 94 °C (denaturation), 30 s at 55 °C (annealing), and 60 s at 72 °C (extension). The reaction products were subsequently run on a 1% agarose (w/v) gel for 1 h at 120 V.

Subcloning—For immunofluorescence, the CH domain, ΔC-term, ΔGAR, and ΔCH constructs were cloned into pEGFP-N1 or mCherry-N1 vectors (Clontech) using the restriction endonucleases NheI and HindIII at the sites indicated in Fig. 1*A*. The other constructs were all cloned into the pEGFP-C1 vector (Clontech) using the restriction endonucleases BspEI and BamHI for GAS2-like 3, EcoRI and BamHI for the GAR domain, and BamHI for the C terminus.

For recombinant expression in *Escherichia coli*, the CH domain and C terminus were cloned into the pHisTrx2 vector (14) using the restriction endonucleases BamHI and EcoRI or BamHI, respectively. The GAR domain was cloned into pHisNusA, a derivative of pET-43 (Invitrogen), using the same restriction sites as for immunofluorescence. All of the recombinant insert DNA was verified by DNA sequencing.

Protein Expression and Purification—The recombinant GAS2-like 3 constructs were expressed in *E. coli* JM109 (DE3) host strain (Merck) as previously described (15) using an autoinduction protocol (as described in Ref. 16). The His_6-tagged proteins were purified by immobilized metal affinity chromatography on Ni^{2+}-Sepharose (GE Healthcare). Purification was performed as described in the pET system manual (Merck).

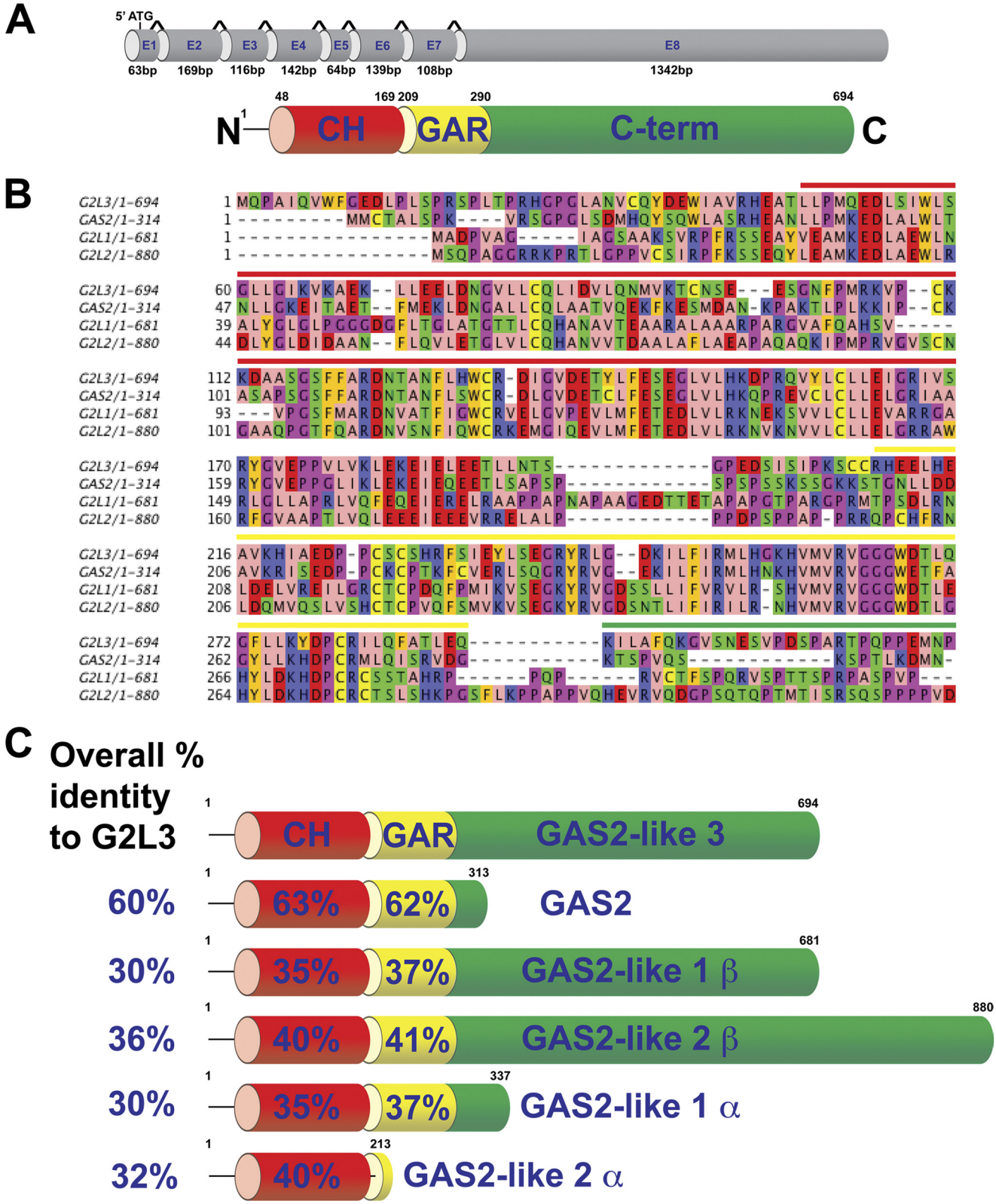

FIGURE 1. **Schematic representation of the intron-exon boundaries of the G2L3 gene and the sequence alignments of the human GAS2 protein family.** *A*, the G2L3 gene consists of eight exons interspersed by seven introns. The CH and GAR domains are depicted in *red* and *yellow*, respectively, and the C terminus (*C-term*) is in *green*. *B*, sequence alignment of the GAS2 family, showing the conservation between the N termini of the GAS2 family members. The *β*-isoforms of G2L1 and G2L2 are shown. Note the high degree of conservation between family members. The *colored bars* above the alignments indicate the domain boundaries of the GAS2 family and are colored according to their domains as in *A*. AAs are illustrated according to their physicochemical properties using the Zappo color scheme. In brief, aliphatic or hydrophobic AAs are *pink*, aromatic AAs are *orange*, positively charged AAs are *red*, negatively charged AAs are *green*, hydrophilic AAs are *blue*, proline/glycine is *magenta*, and cysteine is *yellow*. *C*, the AA percentage identities between G2L3 and the other GAS2 family members are indicated, as well as the percentage identities between the various domains.

Removal of the His_6 tags by thrombin from the CH domain and C terminus was performed as previously described (15). Determination of protein concentration was achieved by the absorbance of tryptophan and tyrosine residues at 280 nm (17).

In Vitro Sedimentation Assays—Actin and MT binding assays were performed using the Non-Muscle Actin Binding Protein Spin-Down Biochem kit and the Microtubule Associated Protein Spin-Down assay kit (both from Cytsokeleton, Inc.), respectively, according to the manufacturer's recommendations. Briefly, the proteins were prespun at 150,000 × *g* at 4 °C for 90 min for the actin binding assay or at 100,000 × *g* at 25 °C for 1 h for the MT binding assay. The proteins were then incubated with the polymerized forms of either F-actin or MTs and centrifuged at 150,000 × *g* at 24 °C for 90 min or at 100,000 × *g* at 25 °C for 40 min, respectively. The supernatants were aspirated and boiled in SDS sample buffer, and the pellets were resuspended in SDS sample buffer. Following which, the samples were analyzed on 10% SDS-PAGE gels for the GAR domain and C terminus, and 15% SDS-PAGE gels were used for the CH domain. All of the protein bands were visualized using Coomassie Blue staining.

Sequence Alignments—Sequence alignments were performed using the program Jalview (18).

Statistical Analysis—Using the ratios obtained from the image processing, Student's *t* tests were performed using Microsoft Excel to compare the ratios of G2L3 expressing control cells and TSA-treated G2L3-expressing cells.

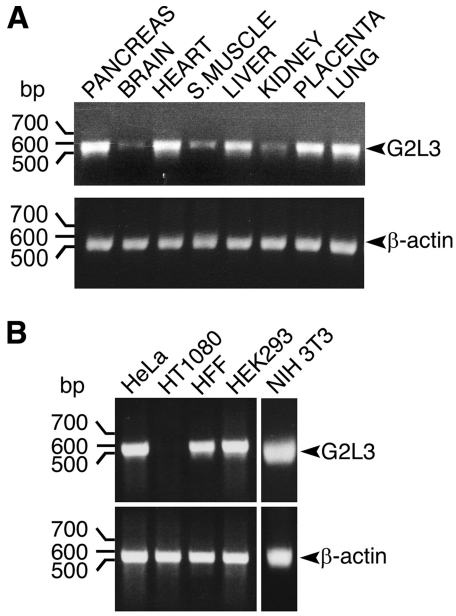

FIGURE 2. **G2L3 is expressed ubiquitously in human tissues and cell lines.** *A*, PCRs were performed on cDNA panels generated from different tissues, using primers specific for G2L3, which spanned exons 2 to 6. Primers designed specifically to recognize β-actin were used as loading controls. *B*, PCRs were performed using cDNA libraries generated from different cell lines. The human tissues, human cell lines (HeLa, HT1080, human foreskin fibroblast (*HFF*), and HEK293) and mouse cell line (NIH3T3) are indicated above each panel, the sizes of DNA are indicated on the *left side* of the panel in bp, and the expected PCR product sizes are indicated by *arrowheads*. Note the low expression of G2L3 in brain tissue and its absence in the HT1080 cell line. The data are representative of three independent experiments.

RESULTS

GAS2-like 3 Is Highly Conserved among Species and Is Widely Expressed in Human Tissues—To identify potential actin and MT-binding proteins, we performed a TBLASTN search for genes containing both CH and GAR domains using GAS2 as a template. As a proof of principle, we identified GAS2, G2L1, G2L2, MACF1, bullous pemphigoid antigen 1, and picked eggs (Pigs), but also an uncharacterized gene, G2L3 (GenBank/EMBL/DDJB accession number AC_000144). It has an open reading frame of 2229 base pairs, spanning eight exons and encodes a putative protein of 694 amino acids (AAs) with a calculated molecular mass of 75.2 kDa (Fig. 1*A*). The protein sequence consists of a single N-terminal CH3 class, CH domain comprising 122 AAs, with 24% AA identity to the CH domain identified in calponin. C-terminal of the CH domain is an 82-AA-long GAR domain, which abuts to a stretch of 404 AAs that is predicted to have little secondary structure. The domain organization of G2L3 is the same as G2L1 and G2L2, therefore classifying it as a new member of the GAS2 protein family.

G2L3 shares the highest AA identity to GAS2 (60%) and the lowest identities with G2L1 and G2L2 at 30 and 36%, respectively (Fig. 1, *B* and *C*). In terms of domain sequence conservation, the CH and GAR domains of G2L3 are compared with the other members in Fig. 1*C*.

G2L3 homologues are present in all vertebrates; for example, there is 65% identity between the conserved CH and GAR domains belonging to the human G2L3 and the zebrafish G2L3 (see supplemental Table S1). There is also evidence for the existence of genes with the same domain architectures in *Drosophila melanogaster*, where it has been named Pigs (accession number NM_132103) (43). A similar gene is expressed in *Caenorhabditis elegans*, where the CH domain has been duplicated (accession number NM_069025). Taken together, we have discovered a new member of the GAS2 family by searching for genes related to GAS2 that is highly conserved through evolution, which implies it plays an important function.

We next sought to determine the expression of G2L3 in human tissues and cell lines. Using cDNA libraries generated from different human tissues and cell lines, we performed PCRs to investigate the respective levels of G2L3 mRNA and used this as an indication of G2L3 protein levels. G2L3 mRNA was widely expressed within the body and was most prominent in the pancreas, heart, liver, placenta, and lung. It was expressed at low levels in the brain, skeletal muscle, and kidney (Fig. 2*A*). Because tissues contain many different cell types, we investigated whether G2L3 expression was confined to a particular one. We discovered G2L3 in a wide variety of cell lines, including HeLa, human foreskin fibroblasts, human embryonic kidney 293 cells, and we found the murine homologue in NIH3T3 cells. Conversely, it was not expressed in HT1080 cells, which are a highly transformed cell line (Fig. 2*B*). These data suggest that G2L3 is abundantly expressed in many tissues and cell lines. Notably, it is absent in HT1080 cells, which may indicate a role in tumor suppression, as described for caveolin-1 (19).

The Calponin Homology Domain Mediates Localization to Actin Stress Fibers and the C Terminus Recruits GAS2-like 3 to Microtubules—To determine the subcellular localization of G2L3 and to study the roles of its domains in this localization,

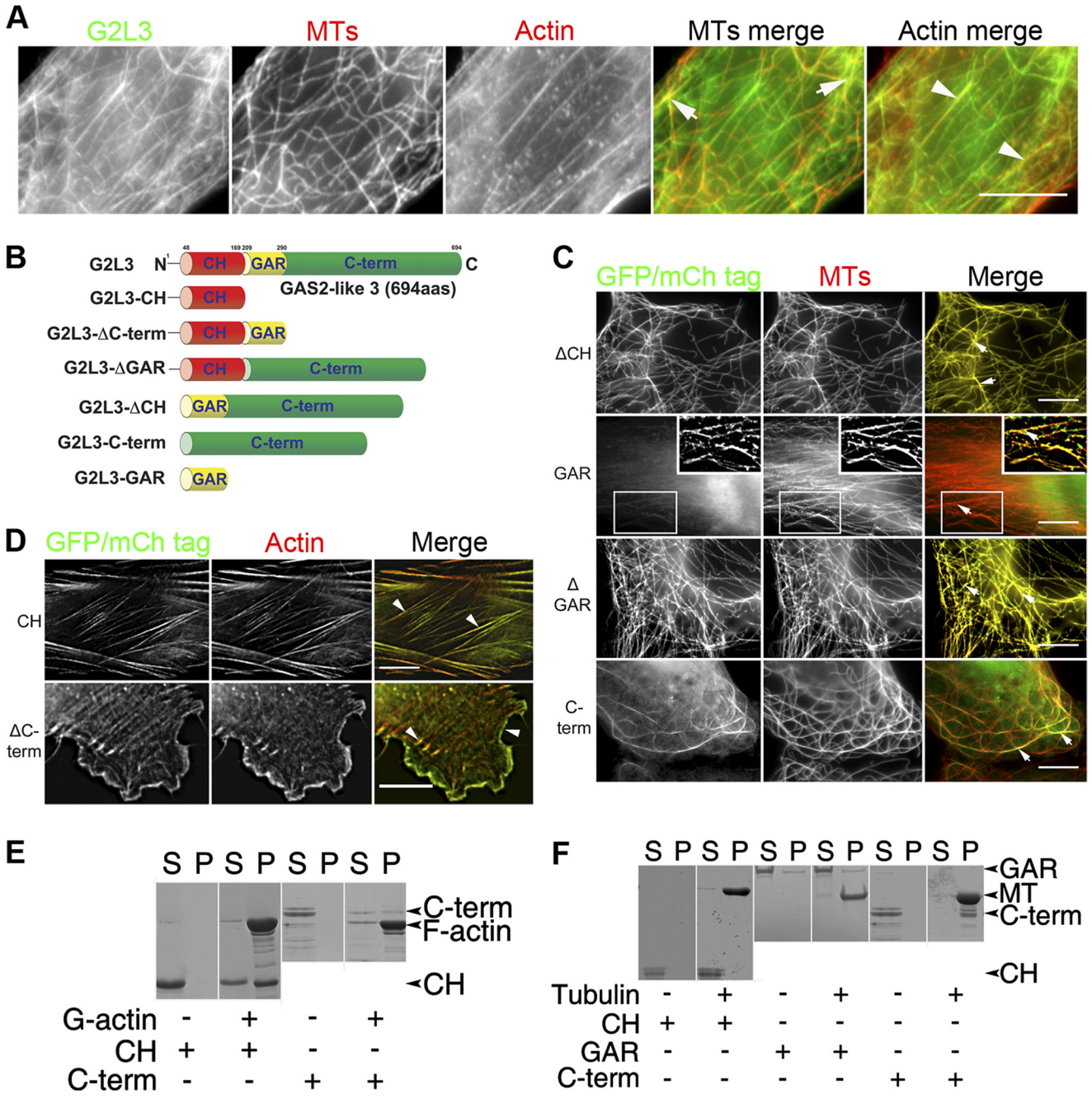

FIGURE 3. **G2L3 binds and localizes to both microtubule and actin cytoskeletons.** *A*, *C*, and *D*, G2L3 constructs were transiently expressed in NIH3T3 cells, followed by fixation and staining using an antibody that recognizes α-tubulin (DM1A) (41) and phalloidin to label actin. *A*, G2L3 localizes to both F-actin (*white arrowheads*) and MT cytoskeletons (*white arrows*). *B*, G2L3 constructs that were expressed as fusion constructs to GFP or mCherry (*mCh*) in NIH3T3 cells. *C*, G2L3-ΔCH (Δ*CH*), G2L3-ΔGAR (Δ*GAR*), and G2L3-C-term (*C-term*) all localize to MTs, and G2L3-GAR (*GAR*) localizes diffusely in the cytoplasm. *D*, G2L3-CH (*CH*) and G2L3-ΔC-term (Δ*C-term*) localize to F-actin structures. *E*, actin binding assays were performed using recombinant versions of G2L3-CH (*CH*) and G2L3-C-term (*C-term*), showing that the CH domain directly binds F-actin, whereas the C-term does not. *F*, MT-spin down assays were performed using G2L3-CH (*CH*) and G2L3-GAR (*GAR*) as well as G2L3-C-term (*C-term*), showing that only G2L3-C-term directly interacts with MTs *in vitro*. The predicted sizes of the proteins are indicated by *arrowheads*. Both immunofluorescence and binding assay data are representative of three independent experiments. *Bars*, 10 μm.

we expressed fluorophore-tagged versions of G2L3 and a series of G2L3 mutants in NIH3T3 cells. We found that full-length G2L3 localized to overlapping MTs and actin stress fibers in 70% of all tested cells and G2L3 localized only to MTs in the remaining 25% of cells (Fig. 3*A*). The localization to actin was mediated by the CH domain, because expression of this domain alone (referred to as G2L3-CH) decorated actin stress fibers in all cells (Fig. 3, *B* and *D*). In contrast, a construct missing the CH domain (G2L3-ΔCH) localized predominantly to MTs, suggesting that the remaining sequence contained a MT-binding site (Fig. 3, *B* and *C*). To our surprise, the localization to MTs was mediated by the C terminus, because expression of this domain (G2L3-C-term) localized exclusively to MTs (Fig. 3*C*). Notably, the MTs appeared to be bundled in 82% of cells expressing G2L3-C-term. To investigate whether the GAR domain, a domain that has been frequently implicated in MT

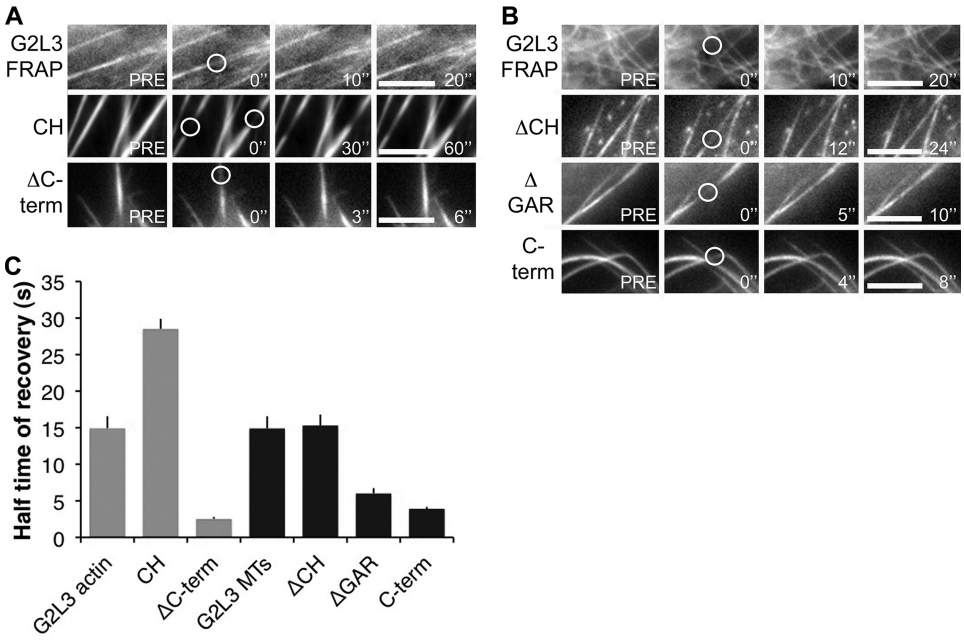

FIGURE 4. **The individual domains of G2L3 influence the binding strength to microtubules and actin.** To assess the turnover of indicated proteins in NIH3T3 cells, circular areas of 1.5-μm diameter were bleached, and recovery was measured. *A*, FRAP experiments performed on the actin localizing constructs. Note the slower fluorescence recovery of bleached areas in G2L3-CH (*CH*)-expressing cells and much faster recovery in G2L3-ΔC-term expressing cells compared with areas in G2L3-expressing cells. *B*, FRAP experiments performed on MT localizing constructs. Note the similar fluorescence recovery of bleached areas in cells expressing G2L3 and G2L3-ΔCH. Conversely, the fluorescence recovers faster in the bleached areas in G2L3-ΔGAR and G2L3-C-term-expressing cells. Either the prebleach (*PRE*) or the time in seconds is indicated in the *bottom right-hand corner* of each image, and the encircled areas indicate the bleach regions. *C*, the $t_{1/2}$ values of recovery of the actin binding constructs are labeled in *gray*, and the MT-binding constructs are in *black*. Note that the $t_{1/2}$ of recovery of G2L3-CH is almost double that of G2L3, and the $t_{1/2}$ of recovery of G2L3-ΔC-term is much faster than G2L3. In accordance with *B*, the $t_{1/2}$ of recovery of G2L3-ΔCH is similar to G2L3, whereas G2L3-ΔGAR and G2L3-C-term have much faster $t_{1/2}$ values of recovery. The data represent the results from more than $n = 20$ bleach regions from $n = 10$ cells and are representative of three independent experiments. *Bars*, 5 μm.

binding in other proteins (7), played a role in localizing G2L3 to either cytoskeleton, we generated mutants including and excluding this domain (G2L3-GAR and G2L3-ΔGAR, respectively) (Fig. 3*B*). We found that G2L3-GAR localized diffusely in the cytoplasm in most cells and G2L3-ΔGAR localized along the MT lattice, implying that the GAR domain is not fundamental for G2L3 localization to MTs or actin (Fig. 3*C*). G2L3-ΔC-term, which lacks the C terminus but contains both the CH and GAR domains, localized predominantly to the actin cytoskeleton but interestingly to different actin structures than G2L3-CH. Specifically, G2L3-ΔC-term localized to both lamellipodia and filopodia (Fig. 3*D*).

Taken together, these data indicate that the CH domain controls the localization of G2L3 to actin and the C terminus regulates its localization to MTs. The GAR domain is not essential for localization to MTs, and the bundling of MTs by the C terminus may imply that it has the ability to cross-link MTs.

GAS2-like 3 Interacts Directly with Microtubules and Filamentous Actin—To determine whether the localization of the individual domains of G2L3 is mediated by direct interactions with the different cytoskeletal systems, we performed *in vitro* cosedimentation assays using recombinant purified domains. We found that purified G2L3-CH cosedimented with F-actin after high speed centrifugation, indicating that there is a direct interaction (Fig. 3*E*). Conversely, the majority of G2L3-C-term remained in the supernatant. A small amount cosedimented with F-actin; however, this is likely through a nonspecific interaction, as has been documented for positively charged peptides (20). Given the exclusive localization of G2L3-C-term to MTs in cells (Fig. 3*C*), we conclude that G2L3-C-term mediates MT binding. As controls, the proteins were centrifuged in the absence of polymerized actin, and both were found in the supernatant, showing they fail to sediment alone. A similar assay was performed with MTs, to reveal that G2L3-C-term interacts directly with MTs (Fig. 3*F*). In contrast, neither G2L3-CH nor G2L3-GAR were found in the pellet fraction with MTs, implying that neither interact directly with MTs (Fig. 3*F*).

Overall, these data are consistent with the immunofluorescence data, confirming that the CH domain binds to actin, and the C terminus binds to MTs. These data suggest that the GAR domain does not interact with MTs directly *in vitro*.

The Individual Domains of GAS2-like 3 Influence the Binding Strength to Microtubules and F-actin—To study the influence of the different domains of G2L3 on its binding strength to F-actin or MTs, we performed FRAP experiments on cells expressing different mutants (Fig. 4, *A* and *B*). In these experiments, we determined the half-time ($t_{1/2}$) of recovery of the different mutants, and used it as an indicator of protein mobility (21, 22). In comparison with the subpopulation of G2L3 which localized to actin, we observed a 2-fold increase in the $t_{1/2}$ of recovery of 28.5 s for G2L3-CH, indicating that the turnover of the CH domain is slower than full-length G2L3 (Fig. 4, *A* and *C*). Conversely, G2L3-ΔC-term showed a 6-fold decrease in $t_{1/2}$ of recovery of 2.5 s compared with G2L3, implying the turnover of G2L3-ΔC-term is faster and has a weaker interaction with actin than G2L3. These data indicate that the removal of the GAR domain and the C terminus amplifies the binding strength of the CH domain for actin. Accordingly, the presence of the GAR

domain alone is sufficient to destabilize the interaction of the CH domain with actin. We subsequently analyzed the mobility of the various constructs that localized to MTs (Fig. 4*B*). We discovered that full-length G2L3 and the construct lacking the CH domain (G2L3-ΔCH) had the slowest turnovers, with $t_{½}$ values of recovery of 14.9 and 15.3 s, respectively. Suggesting that the CH domain does not affect the interaction of G2L3 with MTs. In contrast, the $t_{½}$ of recovery of G2L3-C-term was reduced almost 4-fold (3.9 s), and the $t_{½}$ of recovery of G2L3-ΔGAR was more than halved (6 s) (Fig. 4*C*). These data indicate that the simultaneous removal of both the CH and GAR domains destabilizes the interaction of the C terminus with MTs. In summary, the results suggest a critical role for the GAR domain in modulating the binding to the different cytoskeletal systems, strengthening the interaction with MTs, but weakening the interaction with F-actin.

GAS2-like 3 Localization Is Dependent on Both Microtubule and Actin Cytoskeletons—The localization of G2L3 was variable in cells. In 70% of cells, G2L3 localized to both MTs and F-actin, in 25% of cells it localized exclusively to MTs, and in the remaining 5% it localized diffusely. The cause of this variability is unclear; however, the presence of both MT- and actin-binding sites on G2L3 may provide insights and raises the question whether the interaction of G2L3 with one of the cytoskeletons influences the binding to the other. To elucidate this, we disrupted the actin cytoskeleton using cytochalasin D, which resulted in G2L3 localizing more to MTs (83% compared with 25% in untreated control cells) (Fig. 5). These data suggest that F-actin is not required for G2L3 localization to MTs. After treatment of cells with nocodazole to ablate MTs, G2L3 localized diffusely in many cells (48% compared with 5% in control cells). In a small percentage of cells treated with nocodazole, G2L3 localized to the actin cytoskeleton (7%). Notably, G2L3 localization was enhanced to nocodazole-resistant MTs, in a subset of cells. These data imply that MTs aid G2L3 localization to F-actin; however, they are not fundamental for it. In summary, these data suggest that G2L3 is able to localize independently to both F-actin and MTs; however, the presence of MTs aids G2L3 localization to F-actin.

Post-translational Acetylation of Tubulin Enhances GAS2-like 3 Localization to Microtubules—The enhancement of localization of G2L3 to remnant MTs after nocodazole treatment suggests that G2L3 preferentially binds to stable MTs. One way MTs can be stabilized against nocodazole is through post-translational modifications of tubulin, such as acetylation (23). To examine this possibility, we treated G2L3-GFP-expressing cells with the histone deacetylase 6 inhibitor, TSA, which dramatically increases the amount of acetylated α-tubulin (Fig. 6*A*). This increase in tubulin acetylation led to a small, although significant and reproducible, 9% increase in G2L3 recruitment to MTs in comparison with Me_2SO-treated control cells (Fig. 6, *B* and *D*). This increase was not due to the possible stabilization of MTs by the inhibitor *per se*, because MTs stabilized by taxol were not found to increase G2L3 localization (data not shown).

In summary, these data suggest that G2L3 localization may be regulated by molecular mechanisms that lead to MT acetylation. It is currently unclear as to how tubulin acetylation recruits G2L3 to MTs and adds to the list of proteins that are regulated by post-translational modifications of tubulin.

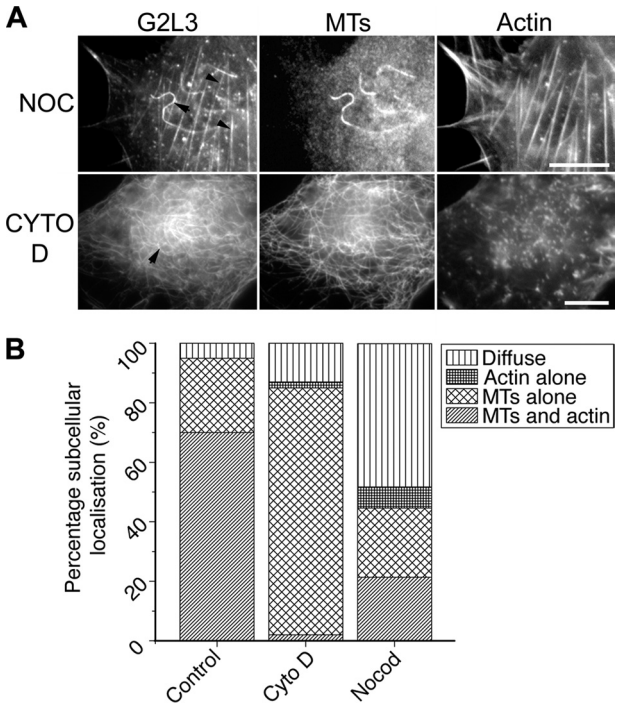

FIGURE 5. **Neither the integrity of actin nor that of microtubules is a prerequisite for G2L3 localization to microtubules or actin cytoskeletons, respectively.** *A*, NIH3T3 cells expressing G2L3 were treated with either 10 μM nocodazole (*NOC*) or 2 μM cytochalasin D (*CYTO D*) for 30 min to determine their effects on G2L3 localization. Note that G2L3 can localize to stable MTs (*top row*, *black arrow*) and actin filaments (*top row*, *black arrowheads*) after NOC treatment, whereas G2L3 predominantly localizes to MTs (*bottom row*, *black arrow*) after treatment of cells with cytochalasin D. *B*, the subcellular localization of G2L3 in cells was quantified after treatment with nocodazole or cytochalasin D. Note that G2L3 localizes diffusely in a greater proportion of cells after NOC treatment, whereas G2L3 localizes to MTs in more cells after cytochalasin D (*Cyto D*) treatment. More than 50 cells were counted for each treatment and are representative of three independent experiments. *Bars*, 10 μm.

DISCUSSION

We have characterized a new member of the GAS2 family, G2L3, that is highly conserved and expressed in many tissues. G2L3 binds to both F-actin and MTs via its single CH domain and unstructured C terminus, respectively. Moreover, we have shown that the GAR domain can modulate the interaction strength of G2L3 with both actin and MTs and that tubulin acetylation enhances G2L3 localization to MTs.

A Single Type 3-Calponin Homology Domain Mediates Actin Binding—Actin-binding of many prominent proteins such as MACF1 and α-actinin is mediated very efficiently by tandem type 1 (CH1) and type 2 (CH2) CH domain repeats (24, 25). The importance of the tandem repeat has been highlighted, because the removal of the CH1 domain in MACF1 ablates its actin binding ability, despite the presence of the remaining CH2 domain (26).

In contrast to the tandem CH1 and CH2 domain repeats, single CH3 domains such as those found in calponin and MT end-binding proteins are considered to be inefficient actin-binding domains (25, 27). It is hypothesized that CH3 domains serve to locate canonical actin-binding domains, for example

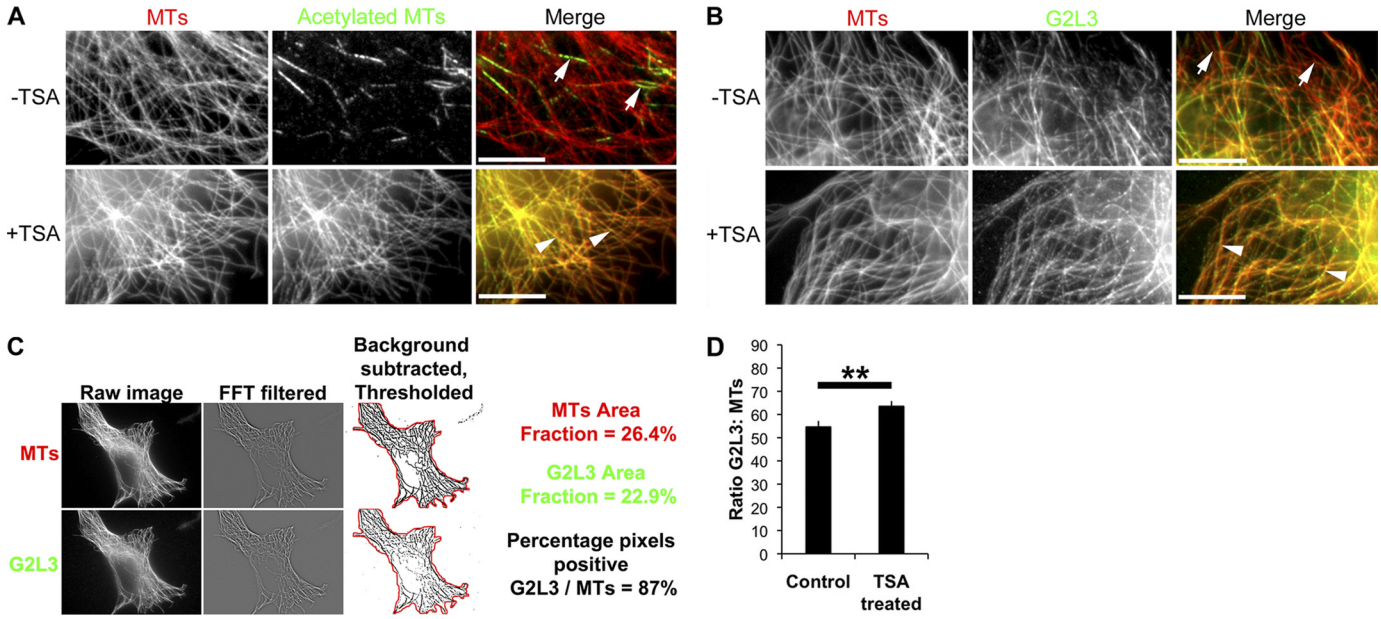

FIGURE 6. **Post-translational acetylation of tubulin enhances G2L3 localization to microtubules.** *A*, NIH3T3 cells were treated with TSA and were fixed and costained using antibodies directed against α-tubulin (DM1A) and acetylated α-tubulin (6–11B-1) (42). Note the low amount of acetylated tubulin in the total MT population in untreated cells (*white arrows*), when compared with TSA-treated cells (*white arrowheads*). *B*, NIH3T3 cells expressing G2L3 were treated with Me_2SO ($-TSA$) or TSA ($+TSA$) and were fixed and stained using the DM1A antibody. Note the enhancement of G2L3 to MTs following TSA treatment (*white arrowheads*) compared with Me_2SO-treated control cells (*white arrows*). *C*, G2L3 and MT images were passed through a FFT two-dimensional bandpass filter and background subtracted. The resulting image was thresholded to MTs, and the cell outline was drawn. Subsequently, the area fraction for G2L3 positive pixels and MTs were recorded, and the ratio between G2L3 and MTs was calculated. *D*, the enhancement of G2L3 to MTs was quantified as in *C*, to show that G2L3 localization was enhanced to MTs after treatment of TSA. More than 50 cells were counted for each condition and are representative of three independent experiments. *Error bars*, S.E. ($p < 0.01$, Student's *t* test). *Bars*, 10 μm.

the CH3 domain on calponin is thought to interact with the CH1 domain on α-actinin and bring it in proximity to actin (28, 29). Despite this evidence, we found that the single CH3 domain in G2L3 does indeed function as an actin-binding domain, an observation that is supported by the other GAS2 family members (2). Interestingly, full-length G2L3 only localizes to actin stress fibers in a subset of cells, implying that the mechanism of CH3 domain binding to actin, in the context of the full-length protein, is tightly regulated. In support of this, our FRAP experiments show lower binding strength to actin when the CH domain is coupled with the GAR domain and may suggest that the latter domain contains a motif that can modulate actin binding. This is further substantiated by F-actin sedimentation assays of G2L2, in which actin was less able to sediment G2L2β than the truncated splice mutant encoding the single CH domain (G2L2α) (2).

The C Terminus Is Essential for Efficient Microtubule Binding—We discovered that the C terminus in G2L3 is fundamental for binding to the MT cytoskeleton and is able to bundle MTs. The highly positively charged C terminus in G2L3 may electrostatically interact with negatively charged MTs, bringing individual MTs together to form MT bundles.

Given the high degree of similarity between the GAR domain in G2L3 and the published MT-binding GAR domains in GAS2 (63% identity) and MACF1 (38%), we predicted that the G2L3-GAR domain would interact with MTs. Conversely to our hypothesis, we found that the GAR domain in G2L3 localizes very weakly to MTs in cells and is unable to bind to them *in vitro*. Our observations are similar to those described for G2L1 and G2L2 (2). This raises an important question as to how the other GAR domains mediate this interaction. Initial sequence analyses revealed that the other GAR domains have overall positive charges, ranging from +2 to +6, whereas the G2L3-GAR has a net charge of zero. Because MTs have an overall negative charge, one likely possibility is that the GAR domains of other proteins interact electrostatically, as has been shown for cationic peptides (30). Further examination of the other GAR domains, based upon the NMR structure of the GAR domain from GAS2, exposed a weakness in construct design. For example, the GAR domain in GAS2 appears to be missing a final methionine residue, which is predicted to form part of the last α-helix (7). Also, the GAR domain used in a recent study on the *Drosophila* spectraplakin, Shot (31), lacks the first four residues, which form part of the initial α-helix. This study showed that the GAR domain localized to MTs very strongly. Both of these published GAR domains are likely to fold incorrectly and may act similarly to the positively charged and unfolded C terminus of G2L3. The comparisons are based upon the NMR structure of the GAR domain from GAS2. Despite these observations, it appears that the G2L3-GAR domain contributes slightly to MT binding strength because our FRAP data suggest that the presence of the GAR domain increases the binding strength of G2L3 to MTs. We speculate that the GAR domain in G2L3, and indeed in other proteins, interacts with MT-associated proteins, which modulate binding to the microtubular network.

Acetylation Contributes to GAS2-like 3 Recruitment to Microtubules—It has been reported previously that detyrosination and acetylation of α-tubulin are hallmarks of MT stabilization (32, 33). We discovered that G2L3 localization to MTs is

enhanced to acetylated MTs, which is similar to other MT-interacting proteins such as the motor protein, kinesin-1 (34, 35). Although the function of this regulation is unclear, parallels can be drawn to the function of tubulin detyrosination. Recently it has been shown that detyrosination of α-tubulin effects the recruitment of proteins that contain a cytoskeleton-associated protein glycine-rich domain (36). Proteins containing these domains include the MT plus end-binding proteins, CLIP-170, and p150glued, which can regulate MT dynamics and targeting. Thus, it is possible that localized tubulin acetylation can drive recruitment of G2L3 to specific loci within the cell, where it then exerts its function.

The Similarity to Spectraplakins—Members of the GAS2 family and the spectraplakins have a similar domain organization, they bind equally to MTs and actin, they both localize similarly in cells, and they exhibit similar behavior in response to cytoskeleton-disrupting drugs (37). These findings strongly suggest they may have similar functions. ACF7 regulates MT growth as well as the dynamics of focal adhesions associated with F-actin (4). Targeting of focal adhesions by MTs is essential for focal adhesion turnover (38), and disrupting MTs leads to inhibition of cell migration (39). MTs grow along F-actin and can thus be guided to adhesion sites (40).[5] In the absence of ACF7, MT growth is unlinked from F-actin in epidermal cells, leading to a diminished turnover rate of focal adhesions and proteins therein (4). Given the potential exciting roles the GAS2 family may play in cell motility, future experiments will be necessary to clarify whether G2L3 or other members of the GAS2 family exert a similar function. With the potential role of stable MTs in migration (33), one possible avenue of investigation will be into the role of tubulin acetylation, and the proteins that mediate this, because they may govern G2L3 function.

Acknowledgments—We are grateful to Dr. Janet Askari for critical reading of the manuscript. We thank Karolina Zielinska (Cambridge) for technical assistance. We thank Peter March and the members of the Faculty of Life Sciences Bioimaging core facility for the help with various microscopes.

REFERENCES

1. Li, R., and Gundersen, G. G. (2008) *Nat. Rev. Mol. Cell. Biol.* **9,** 860–873
2. Goriounov, D., Leung, C. L., and Liem, R. K. (2003) *J. Cell Sci.* **116,** 1045–1058
3. Kodama, A., Karakesisoglou, I., Wong, E., Vaezi, A., and Fuchs, E. (2003) *Cell* **115,** 343–354
4. Wu, X., Kodama, A., and Fuchs, E. (2008) *Cell* **135,** 137–148
5. Jefferson, J. J., Leung, C. L., and Liem, R. K. (2004) *Nat. Rev. Mol. Cell. Biol.* **5,** 542–553
6. Sonnenberg, A., and Liem, R. K. (2007) *Exp. Cell Res.* **313,** 2189–2203
7. Sun, D., Leung, C. L., and Liem, R. K. (2001) *J. Cell Sci.* **114,** 161–172
8. Schneider, C., King, R. M., and Philipson, L. (1988) *Cell* **54,** 787–793
9. Brancolini, C., Bottega, S., and Schneider, C. (1992) *J. Cell Biol.* **117,** 1251–1261
10. Brancolini, C., and Schneider, C. (1994) *J. Cell Biol.* **124,** 743–756
11. Lee, K. K., Tang, M. K., Yew, D. T., Chow, P. H., Yee, S. P., Schneider, C., and Brancolini, C. (1999) *Dev. Biol.* **207,** 14–25
12. Brancolini, C., Benedetti, M., and Schneider, C. (1995) *EMBO J.* **14,** 5179–5190
13. Zucman-Rossi, J., Legoix, P., and Thomas, G. (1996) *Genomics* **38,** 247–254
14. Kammerer, R. A., Schulthess, T., Landwehr, R., Lustig, A., Fischer, D., and Engel, J. (1998) *J. Biol. Chem.* **273,** 10602–10608
15. Kammerer, R. A., Antonsson, P., Schulthess, T., Fauser, C., and Engel, J. (1995) *J. Mol. Biol.* **250,** 64–73
16. Studier, F. W. (2005) *Protein Expr. Purif.* **41,** 207–234
17. Edelhoch, H. (1967) *Biochemistry* **6,** 1948–1954
18. Clamp, M., Cuff, J., Searle, S. M., and Barton, G. J. (2004) *Bioinformatics* **20,** 426–427
19. Wiechen, K., Sers, C., Agoulnik, A., Arlt, K., Dietel, M., Schlag, P. M., and Schneider, U. (2001) *Am. J. Pathol.* **158,** 833–839
20. Wohnsland, F., Schmitz, A. A., Steinmetz, M. O., Aebi, U., and Vergéres, G. (2000) *J. Biol. Chem.* **275,** 20873–20879
21. Carisey, A., Stroud, M., Tsang, R., and Ballestrem, C. (2011) *Methods Mol. Biol.,* in press
22. Humphries, J. D., Wang, P., Streuli, C., Geiger, B., Humphries, M. J., and Ballestrem, C. (2007) *J. Cell Biol.* **179,** 1043–1057
23. Gundersen, G. G., Kim, I., and Chapin, C. J. (1994) *J. Cell Sci.* **107,** 645–659
24. Röper, K., Gregory, S. L., and Brown, N. H. (2002) *J. Cell Sci.* **115,** 4215–4225
25. Gimona, M., Djinovic-Carugo, K., Kranewitter, W. J., and Winder, S. J. (2002) *FEBS Lett.* **513,** 98–106
26. Lee, S., and Kolodziej, P. A. (2002) *Development* **129,** 1195–1204
27. Gimona, M., and Mital, R. (1998) *J. Cell Sci.* **111,** 1813–1821
28. Leinweber, B. D., Leavis, P. C., Grabarek, Z., Wang, C. L., and Morgan, K. G. (1999) *Biochem. J.* **344,** 117–123
29. Galkin, V. E., Orlova, A., Fattoum, A., Walsh, M. P., and Egelman, E. H. (2006) *J. Mol. Biol.* **359,** 478–485
30. Wolff, J. (1998) *Biochemistry* **37,** 10722–10729
31. Applewhite, D. A., Grode, K. D., Keller, D., Zadeh, A., Slep, K. C., and Rogers, S. L. (2010) *Mol. Biol. Cell* **21,** 1714–1724
32. Webster, D. R., and Borisy, G. G. (1989) *J. Cell Sci.* **92,** 57–65
33. Gundersen, G. G., and Bulinski, J. C. (1988) *Proc. Natl. Acad. Sci. U.S.A.* **85,** 5946–5950
34. Reed, N. A., Cai, D., Blasius, T. L., Jih, G. T., Meyhofer, E., Gaertig, J., and Verhey, K. J. (2006) *Curr. Biol.* **16,** 2166–2172
35. Dompierre, J. P., Godin, J. D., Charrin, B. C., Cordelières, F. P., King, S. J., Humbert, S., and Saudou, F. (2007) *J. Neurosci.* **27,** 3571–3583
36. Mishima, M., Maesaki, R., Kasa, M., Watanabe, T., Fukata, M., Kaibuchi, K., and Hakoshima, T. (2007) *Proc. Natl. Acad. Sci. U.S.A.* **104,** 10346–10351
37. Karakesisoglou, I., Yang, Y., and Fuchs, E. (2000) *J. Cell Biol.* **149,** 195–208
38. Kaverina, I., Krylyshkina, O., and Small, J. V. (1999) *J. Cell Biol.* **146,** 1033–1044
39. Ballestrem, C., Wehrle-Haller, B., Hinz, B., and Imhof, B. A. (2000) *Mol. Biol. Cell* **11,** 2999–3012
40. Rodriguez, O. C., Schaefer, A. W., Mandato, C. A., Forscher, P., Bement, W. M., and Waterman-Storer, C. M. (2003) *Nat. Cell Biol.* **5,** 599–609
41. Blose, S. H., Meltzer, D. I., and Feramisco, J. R. (1984) *J. Cell Biol.* **98,** 847–858
42. LeDizet, M., and Piperno, G. (1991) *Methods Enzymol.* **196,** 264–274
43. Pines, M. K., Housden, B. E., Bernard, F., Bray, S. J., and Roper, K. (2010) *Development* **137,** 913–922

[5] M. J. Stroud, R. A. Kammerer, and C. Ballestrem, unpublished observations.